

Supporting Information

Cu encapsulated in hierarchical MFI zeolites for the ethanol dehydrogenation to acetaldehyde

Kachaporn Saenluang^a, Narasiri Mainewaklang^a, Anittha Prasertsab^a,
Tawan Sooknoi^c, Søren Kegnæs^{b,*} and Chularat Wattanakit^{a,*}

^aDepartment of Chemical and Biomolecular Engineering, School of Energy Science and Engineering, Vidyasirimedhi Institute of Science and Technology, Rayong 21210, Thailand.

^bDTU Chemistry, Technical University of Denmark, 2800 Kgs, Lyngby, Denmark.

^cDepartment of Chemistry, School of Science, King Mongkut's Institute of Technology Ladkrabang, Chalongkrung Road, Ladkrabang, Bangkok 10520, Thailand.

* Correspondence: chularat.w@vistec.ac.th and skk@kemi.dtu.dk

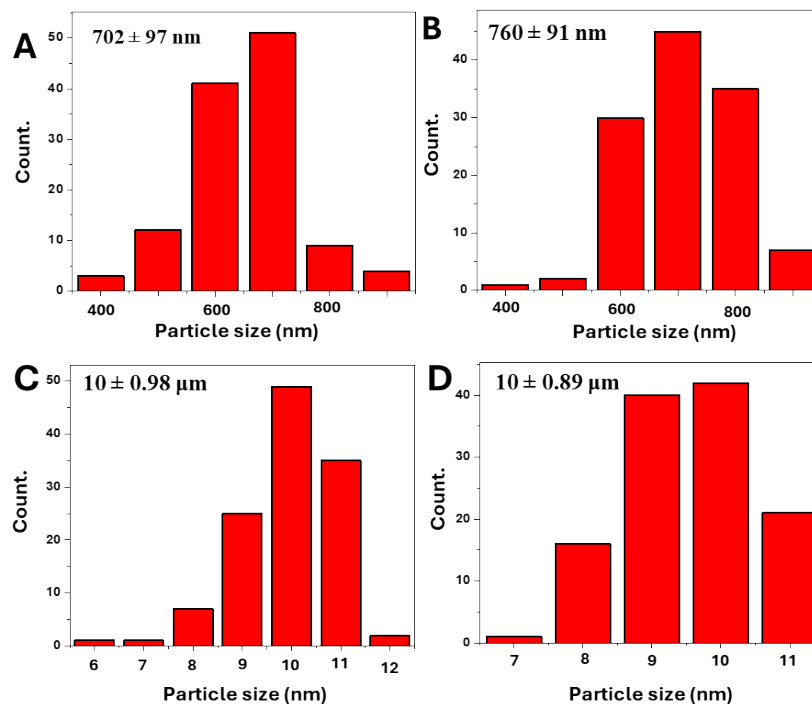


Figure S1. Particle size distribution of (A) Cu@hieZSM-5, (B) Cu@hieS-1, (C) Cu@hieZSM-5, and (D) Cu@conZSM-5. The particle size distribution was determined by counting approximately 100 particles in each sample from SEM images.

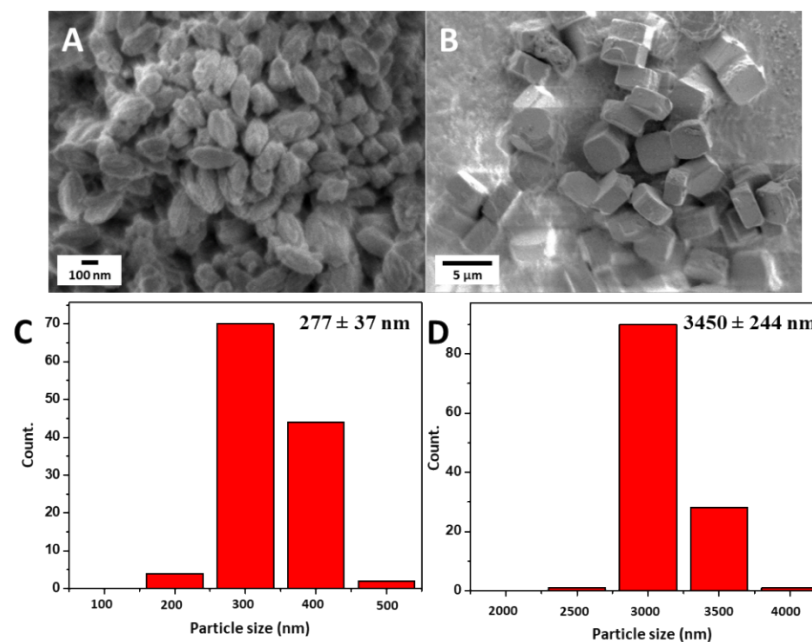


Figure S2. SEM images of (A) hieZSM-5 and (B) conZSM-5 and Particle size distribution of (C) hieZSM-5 and (D) conZSM-5. The particle size distribution was determined by counting approximately 100 particles in each sample from SEM images.

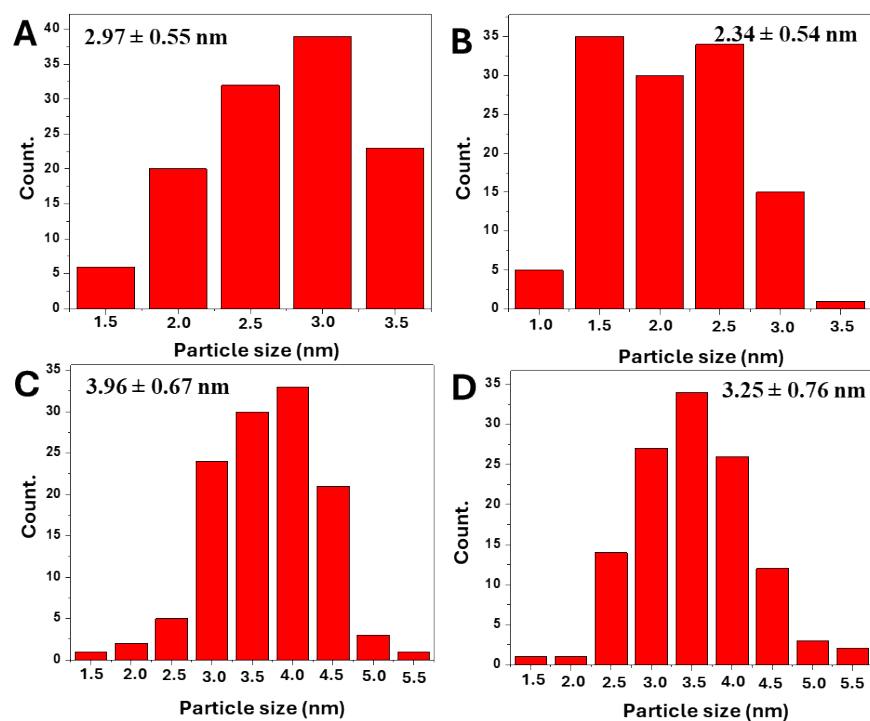


Figure S3. Cu nanoparticles size distribution of (A) Cu@hieZSM-5, (B) Cu@hieS-1, (C) Cu@conZSM-5, and (D) Cu@conS-1. The Cu nanoparticle size distribution was determined by counting approximately 100 particles in each sample from TEM images.

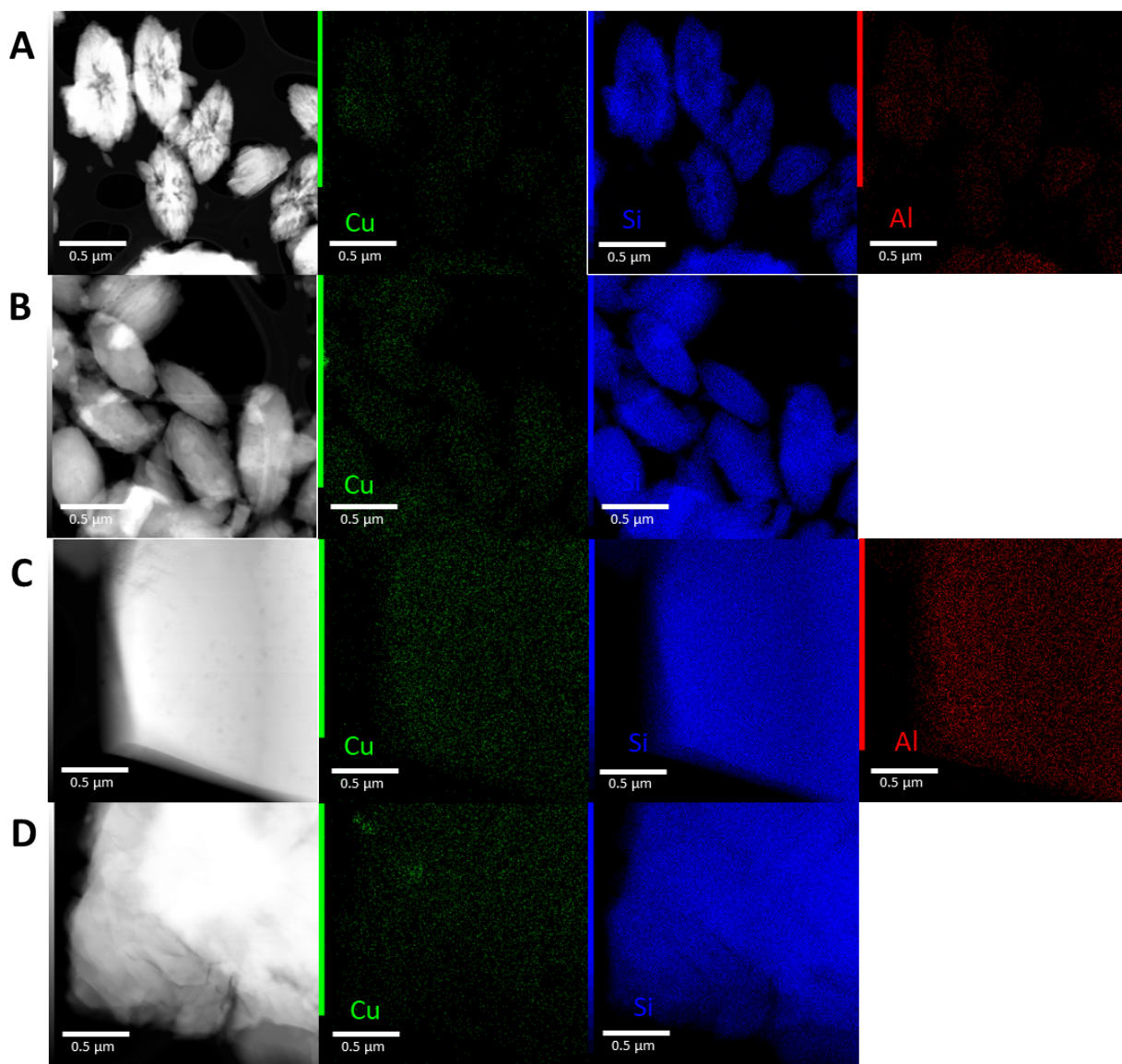


Figure S4. TEM-EDS of (A) Cu@hieZSM-5, (B) Cu@hieS-1, (C) Cu@conZSM-5, and (D) Cu@conS-1.

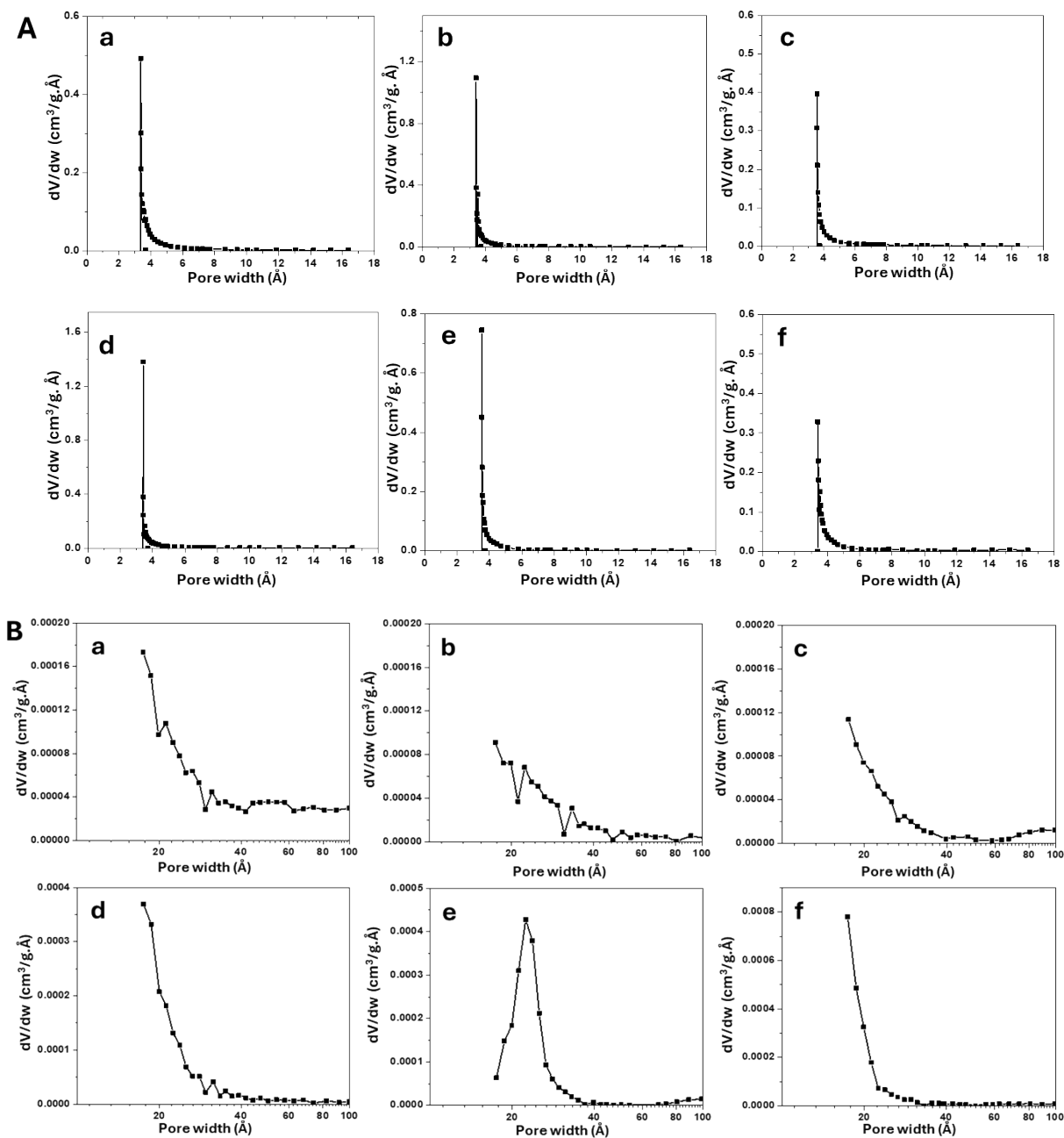


Figure S5. (A) Horvath-Kawazoe (HK) and (B) Barrett-Joyner-Halenda (BJH) pore size distribution, of (a) Cu@hieZSM-5, (b) Cu@hieS-1, (c) hieZSM-5, (d) Cu@conZSM-5, (e) Cu@conS-1, and (f) conZSM-5.

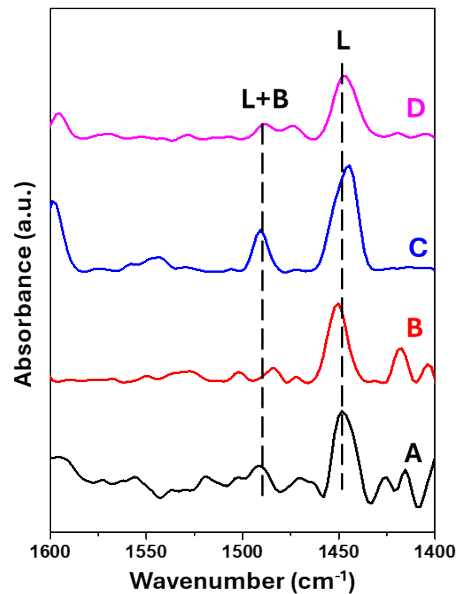


Figure S6. Pyridine-adsorption FTIR curves of (A) Cu@hieZSM-5, (B) Cu@hieS-1, (C) Cu@conZSM-5, and (D) Cu@conS-1.

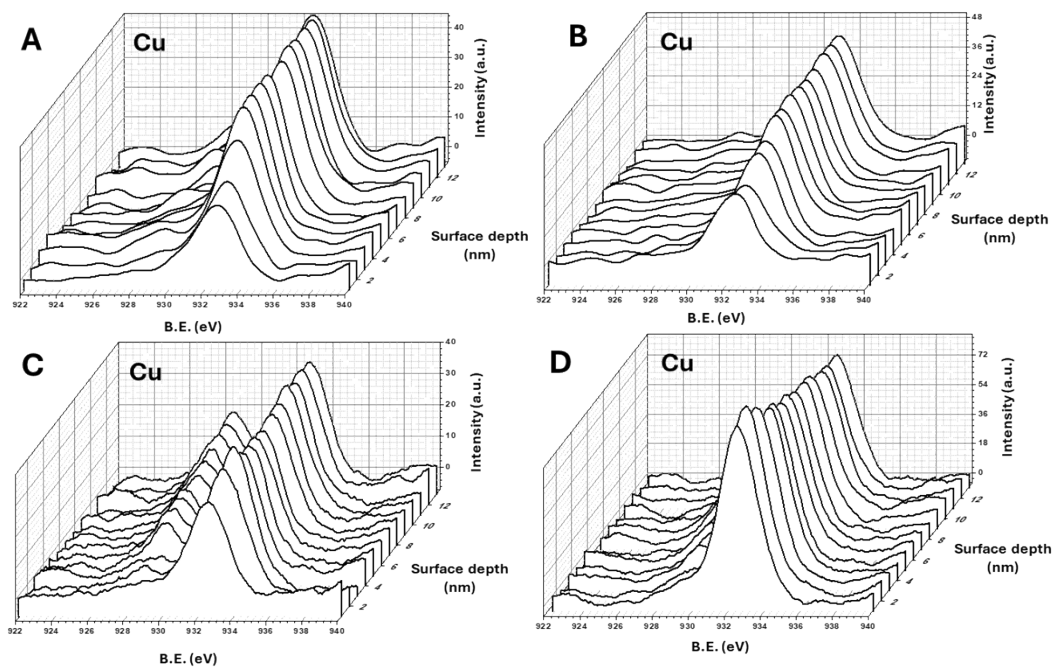


Figure S7. XPS depth profile analysis of the Cu species of (A) Cu@hieZSM-5, (B) Cu@hieS-1, (C) Cu@conZSM-5, and (D) Cu@conS-1.

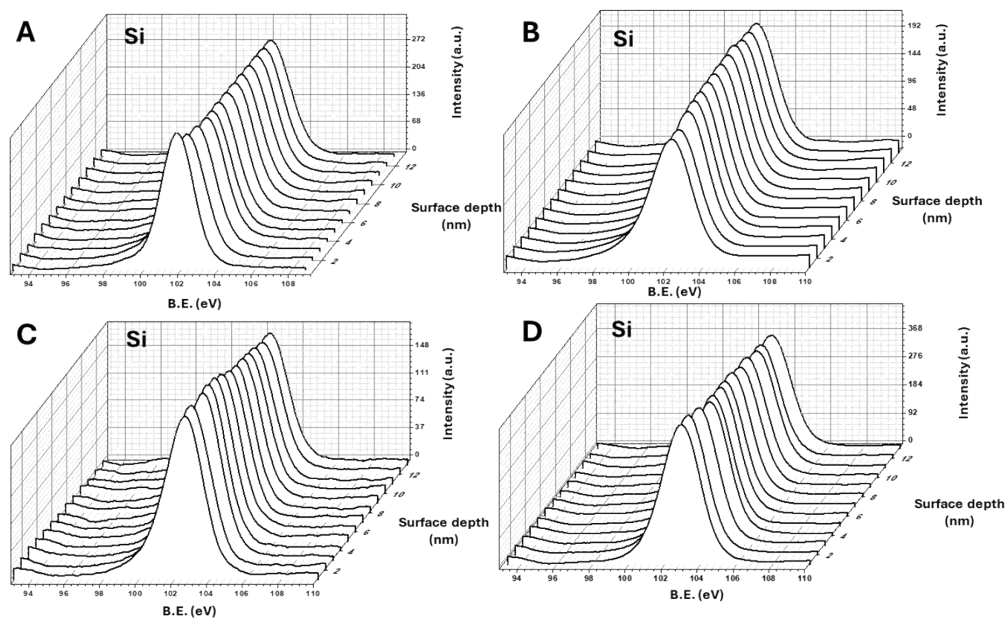


Figure S8. XPS depth profile analysis of Si species (A) Cu@hieZSM-5, (B) Cu@hieS-1, (C) Cu@conZSM-5, and (D) Cu@conS-1.

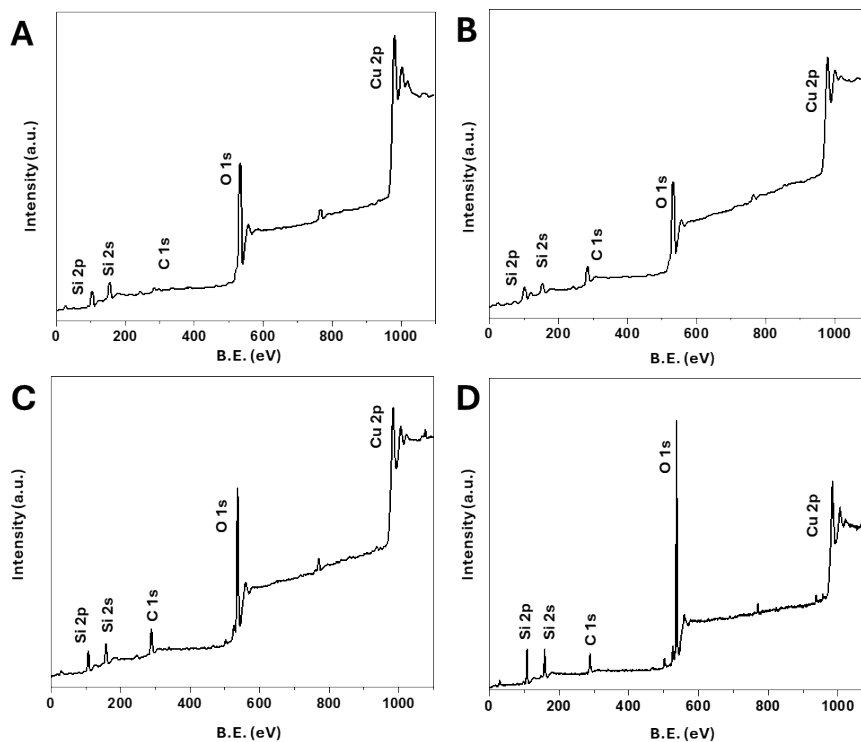


Figure S9. XPS spectra in wide scan (A) Cu@hieZSM-5, (B) Cu@hieS-1, (C) Cu@conZSM-5, and (D) Cu@conS-1.

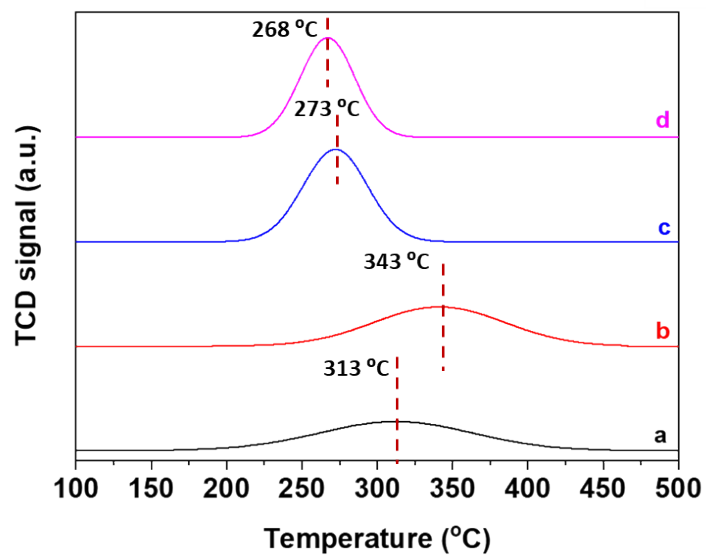


Figure S10. H₂-TPR analysis of (A) Cu@hieZSM-5, (B) Cu@hieS-1, (C) Cu@conZSM-5, and (D) Cu@conS-1.

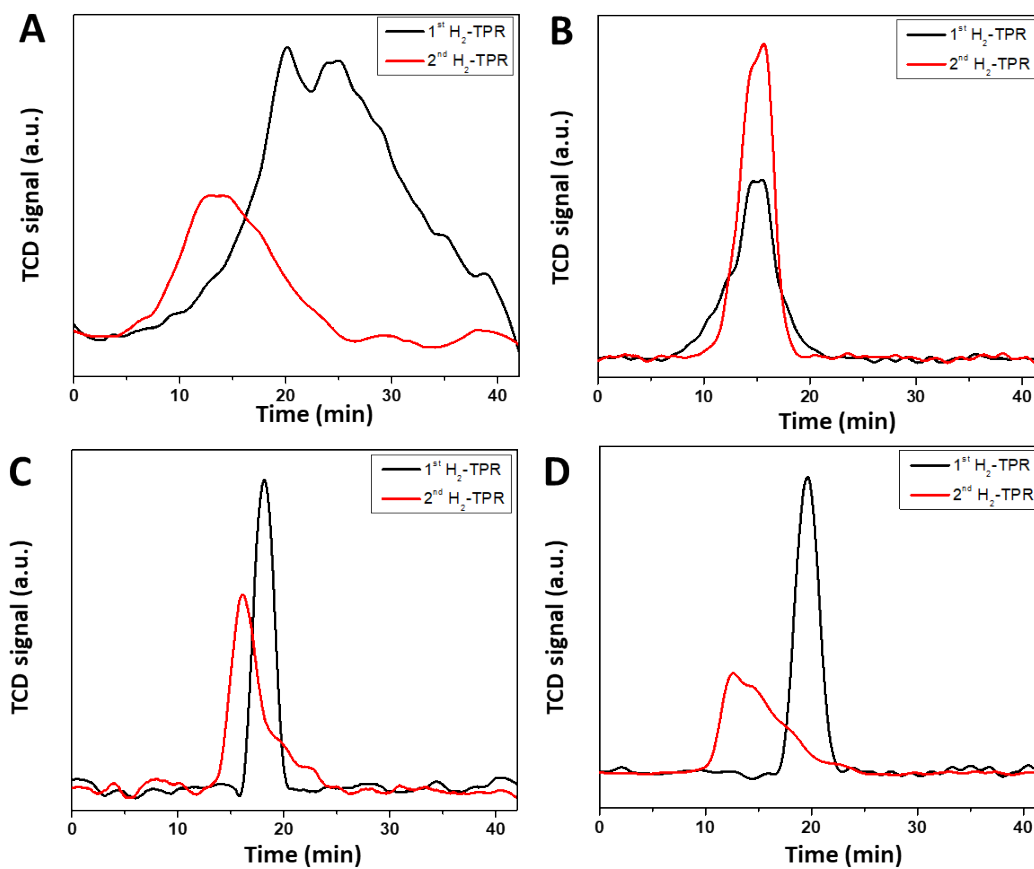


Figure S11. Cu dispersion derived by H₂/N₂O-TPR profiles of (A) Cu@hieZSM-5, (B) Cu@hieS-1, (C) Cu@conZSM-5, and (D) Cu@conS-1.

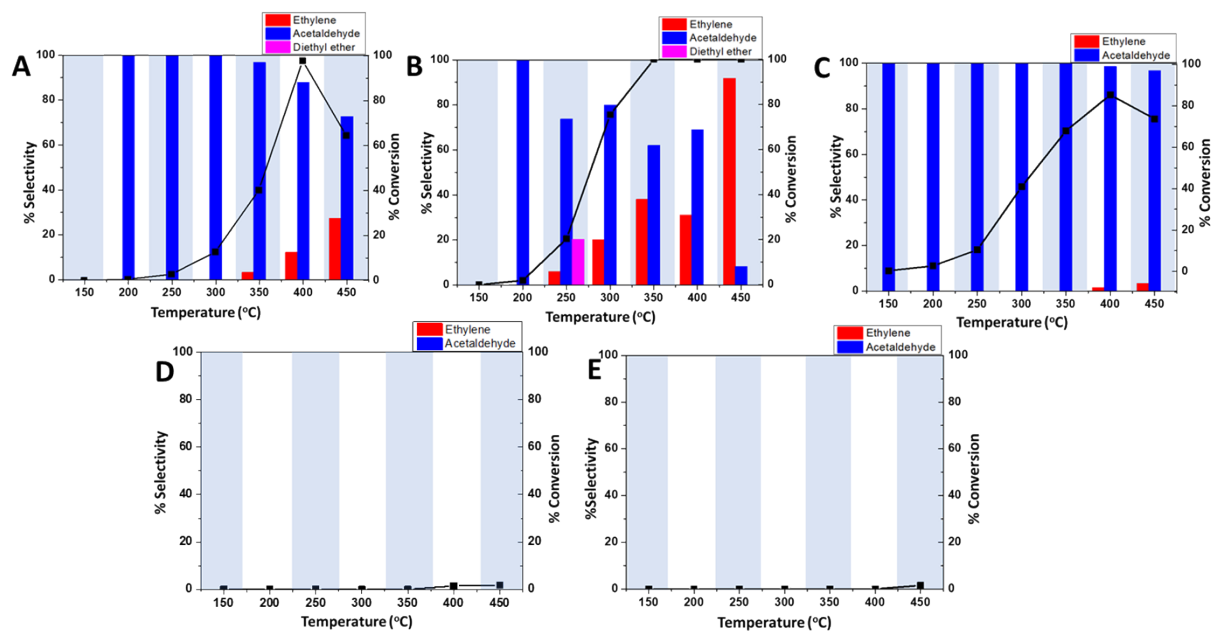


Figure S12. 10%wt ethanol conversion (%) and product selectivities (%) by varying reaction temperature of (A) Cu@hieZSM-5, (B) Cu@conZSM-5, (C) Cu@conS-1, (D) hieZSM-5, and (E) conZSM-5. Condition: 0.1g of catalyst was treated in 10% H_2 gas, a flow rate of reactant 0.04 ml/min, and 50 ml/min of N_2 gas.

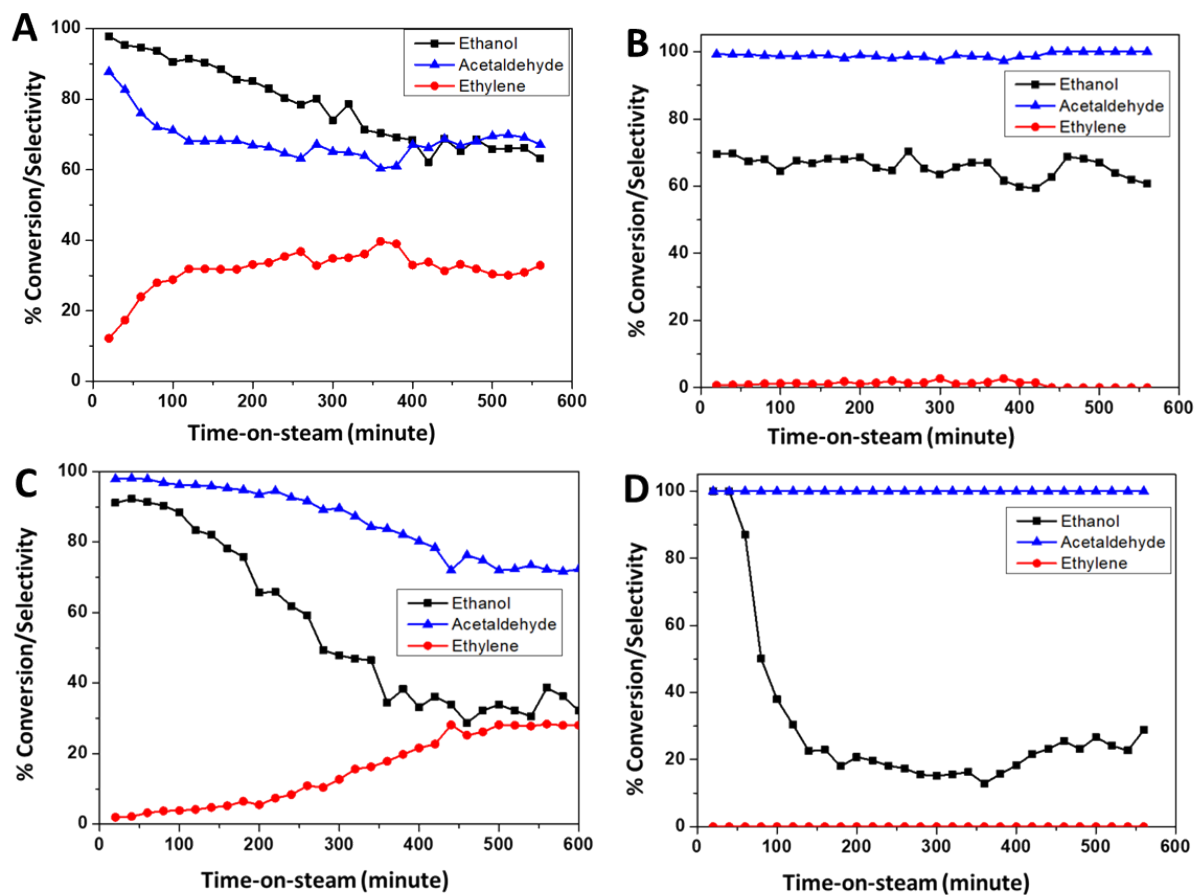


Figure S13. The catalytic stability of 10%wt ethanol as a reactant over (A) Cu@hieZSM-5, (B) Cu@hieS-1, (C) Cu@conZSM-5, and (D) Cu@conS-1. Condition: 0.1g of catalyst was treated in 10% H_2 gas, a flow rate of reactant 0.04 ml/min, and 50 ml/min of N_2 gas at 400°C.

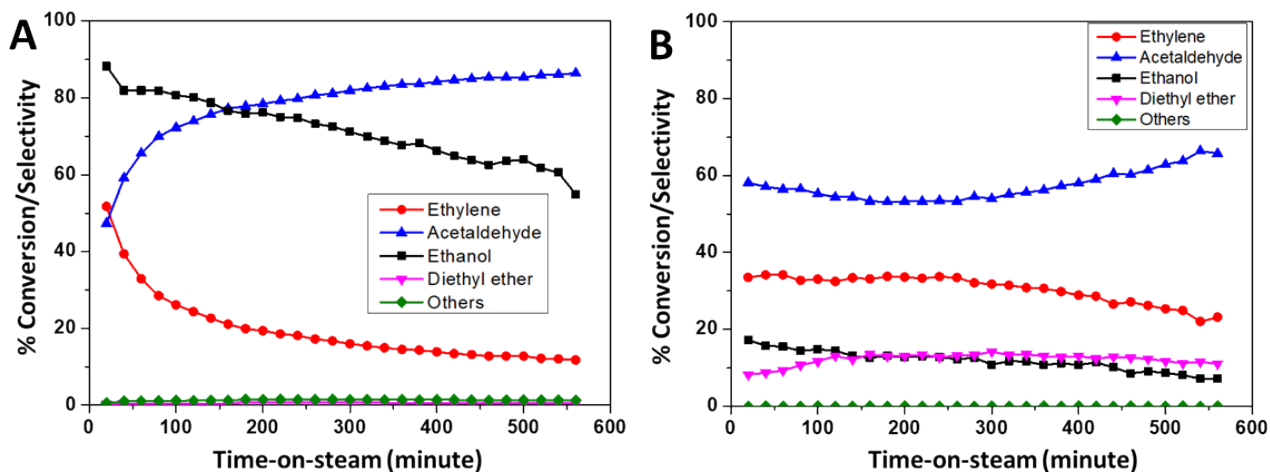


Figure S14. The catalytic stability of absolute ethanol as a reactant as a reactant over (A) Cu@hieZSM-5 and (B) Cu@conZSM-5. Condition: 0.1g of catalyst was treated in 10% H_2 gas, a flow rate of reactant 0.04 ml/min, and 50 ml/min of N_2 gas at 400°C.

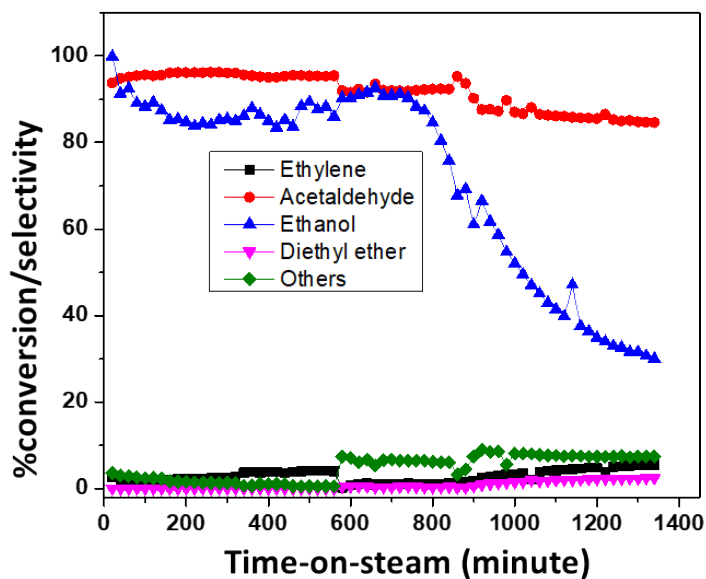


Figure S15. The catalytic stability of absolute ethanol as a reactant as a reactant over Cu@hieS-1 sample. Condition: 0.1g of catalyst was treated in 10% H_2 gas, a flow rate of reactant 0.04 ml/min, and 50 ml/min of N_2 gas at 400°C.

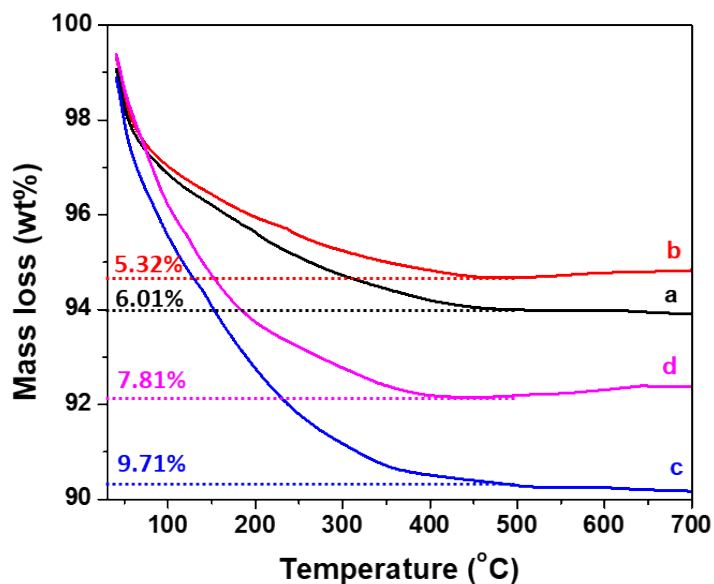


Figure S16. Thermogravimetric analysis (TGA) data of spent catalyst of (A) Cu@hieZSM-5, (B) Cu@hieS-1, (C) Cu@conZSM-5, and (D) Cu@conS-1. Reaction condition: 0.1g of catalyst was treated in 10%H₂ gas, a pure ethanol flow rate of reactant of 0.04 ml/min with 50 ml/min of N₂ gas at 400°C for 300 minutes.

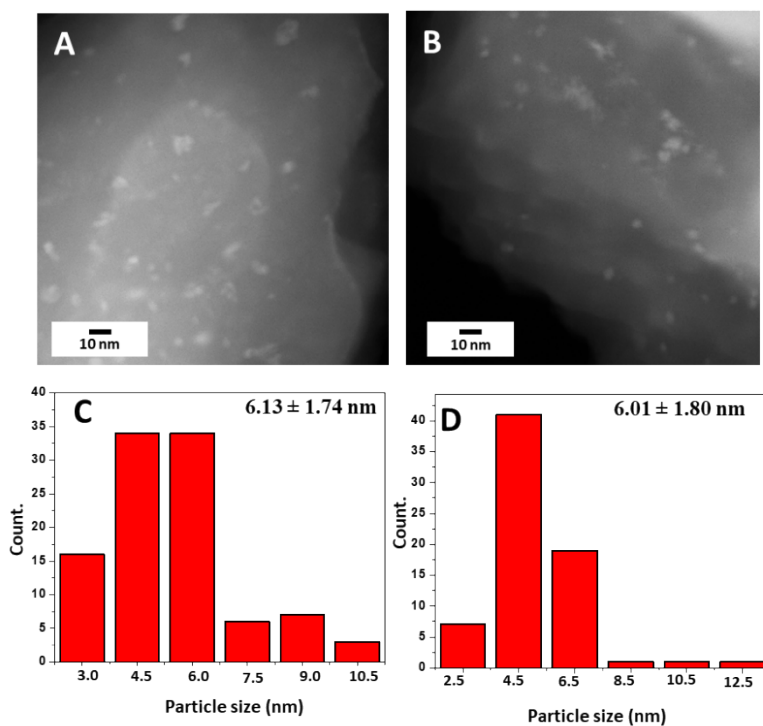


Figure S17. STEM images of (A) Cu@hieS-1 and (B) Cu@conS-1 and Cu nanoparticle size distribution after the reaction over (C) Cu@hieS-1 and (D) Cu@conS-1. The Cu nanoparticle size distribution was determined by counting approximately 100 particles in each sample from SEM images.

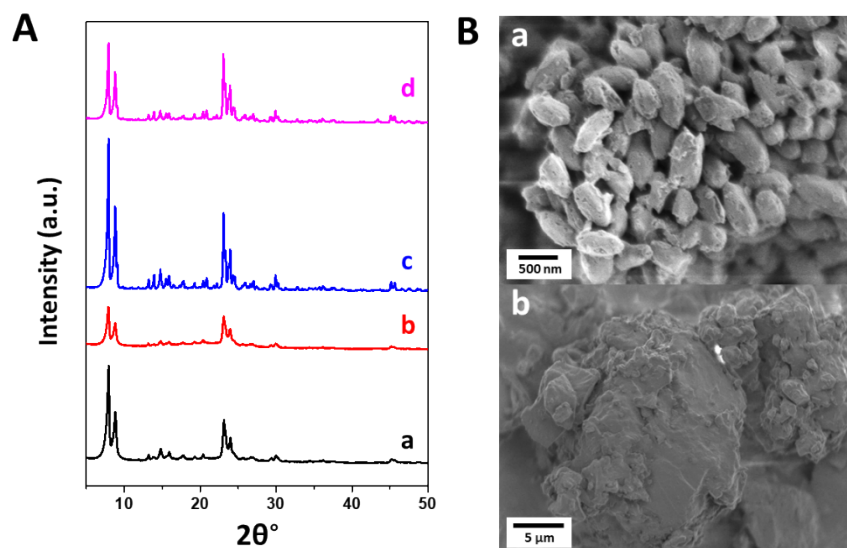


Figure S18. (A) XRD patterns (a) fresh-Cu@hieS-1, (b) spent-Cu@hieS-1, (c) fresh-Cu@conS-1, and (d) spent-Cu@conS-1 and (B) SEM images of (a) spent-Cu@hieS-1 and spent-Cu@conS-1.

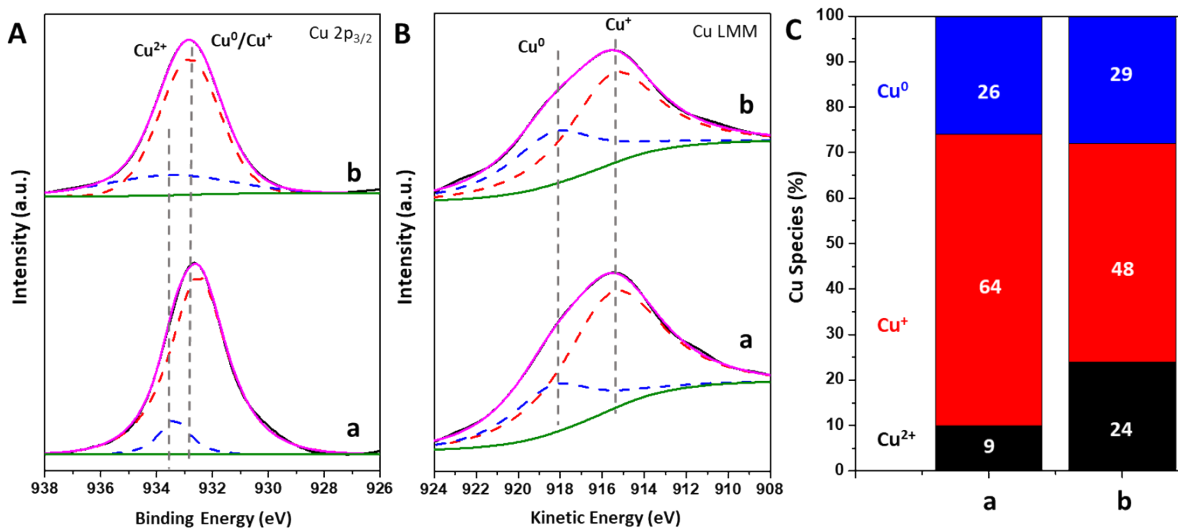


Figure S19. XPS spectra at (A) Cu 2p_{3/2}, (B) Cu LMM Auger region, and (C) content of different Cu species determined by Cu 2p_{3/2} XPS and Cu LMM spectra area of spent catalyst of (a) Cu@hieS-1, and (b) Cu@conS-1.

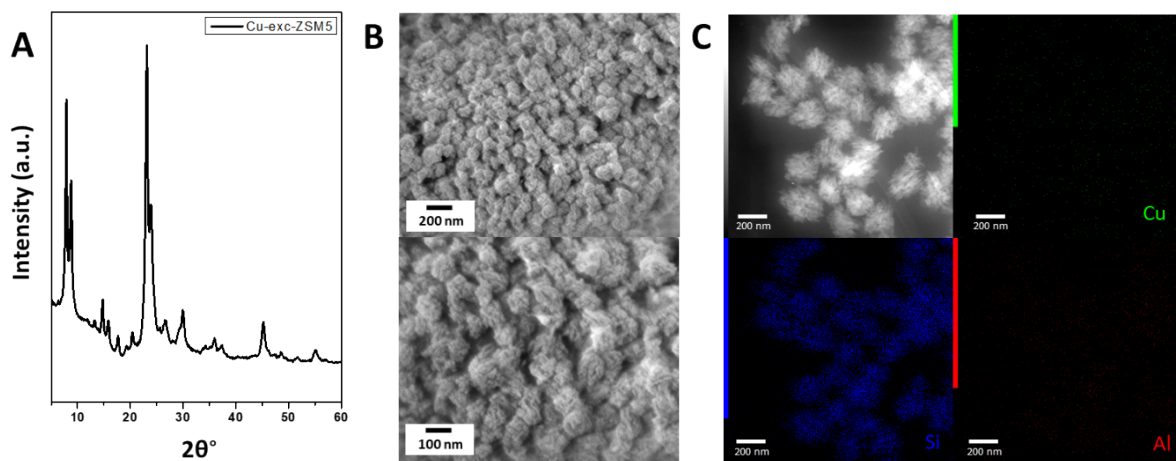


Figure S20. (A) XRD pattern, (B) SEM image, (C) TEM image (D) Si, Al, and Cu elemental mappings of Cu-exc-ZSM5 sample. The Cu content 1.2% was measured by XRF.

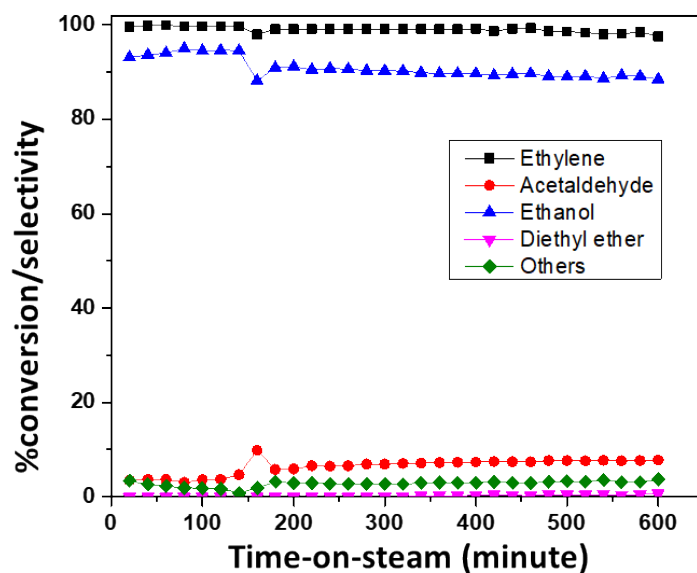


Figure S21. The catalytic stability of absolute ethanol as a reactant as a reactant over the comparable Cu-exc-ZSM5 samples. Condition: 0.1g of catalyst was treated in 10% H_2 gas, a flow rate of reactant 0.04 ml/min, and 50 ml/min of N_2 gas at 400°C.

Table S1. Copper Dispersion and Turnover frequency of four catalysts.

Sample	D _{cu} ^a	TOF (h ⁻¹) ^b
Cu@hieZSM-5	68.6	337
Cu@hieS-1	82.6	1331
Cu@conZSM-5	55.7	349
Cu@conS-1	73.5	95

^aCu dispersion (D_{cu}) was measured by H₂-TPR with N₂O titration and estimated by $(2 \times A2/A1) \times 100\%$ [A2 is the second H₂ consumption and A1 is the first H₂ consumption] and ^bTurnover frequency (TOF) was calculated by the following equation: acetaldehyde yield/(mol of active site×time)

Table S2. Turnover frequency (TOF) of the forward ethanol dehydrogenation reaction on different catalysts.

Reactant	product	Catalyst	Temp. (°C)	TOF ^a (1/h)	Ref.
ethanol	acetaldehyde	Cu@hieS-1	400	1331	The present work
ethanol	acetaldehyde	Cu/Beta	400	10.1	D. Yu, W. Dai, et al. Chinese J, Catal. 2019, 40, 9, 1375-1384
ethanol	acetaldehyde	Cu-MFI-AE	300	6.6	J. Pang, M. et al. ACS Catalysis 2020 10, 22, 13624-13629
ethanol	acetaldehyde	3Cu/NMC	260	48.1	R. Pulikkal Thumbayil, D. B. Christensen, J. Mielby and S. Kegnæs ChemCatChem 2020 12, 22, 5644-5655
ethanol	acetaldehyde	Cu@S-1	250	64.9	L. Lin, et al. J. Catal. 2022, 413, 565-574

^aTurnover frequency (TOF) was calculated by the following equation: acetaldehyde yield/(mol of active site×time)